



FRANCE_CANNES 15-18 SEPT 25

THE FUTURE IS SCIENCE

ifsc2025.com



SOCIÉTÉ FRANÇAISE DE
COSMÉTOLOGIE



IFSCC 2025 full paper (IFSCC2025-277)

"Coffea bengalensis-derived extracellular vesicles: microRNA-mediated modulation of Skin inflammation and neuron communication"

Annalisa Tito^{*1}, Chiara Niespolo¹, Francesca Morra¹, Luciano Pirone², Danilo Mladenovic³, Francesca Loria³, Vincenzo Fogliano^{1,4} and Maria Gabriella Colucci^{1,5}

¹Arterra Bioscience spa, Naples, Italy; ²IBB CNR, Naples, Italy, ³HansaBioMed, Life Sciences Ltd, Tallinn, Estonia; ⁴Wageningen University, Wageningen, Netherlands; ⁵Vitalab srl, Naples, Italy.

1. Introduction

The skin acts as a protective barrier and sensory interface, maintaining dynamic two-way communication with the central nervous system via the skin-brain axis. This interaction allows psychological stress to impact skin physiology through neuroendocrine pathways, while sensory neurons relay environmental stress signals back to the CNS [1]. A key mechanism in this crosstalk is neurogenic inflammation, driven by neuropeptides like CGRP, which activate immune and vascular responses [2]. Cytokines such as IL-33 and IL-6 released by keratinocytes amplify inflammation [3], with Galectin-3 – a β -galactoside binding lectin - further modulating neuroimmune signaling through effects on cytokine release and tissue remodeling [4]. Given the complexity of these pathways, natural compounds that modulate skin-brain communication offer promising therapeutic potential for treating inflammatory and sensitive skin conditions.

Recently, plant-derived extracellular vesicles have gained interest in this field as they are rich in bioactive molecules, including small non-coding RNAs, specialized in intercellular signaling and communication [5]. However, the impact of plant exosomes on skin-brain axis remains unexplored. This study aimed to isolate extracellular vesicles from *Coffea bengalensis* cell culture media and characterize their potential roles in skin regeneration and in modulating interactions between epithelial and neuronal cells involved in neurogenic inflammation.

2. Materials and Methods

EV isolation and purification: Cell culture media from *Coffea bengalensis* cultures, obtained and maintained as described by Bimonte et al [6], were precleared by centrifugation at 10000 r.c.f. for 30 min at RT. The recovered supernatant was subsequently subjected to automated tangential flow filtration (TFF), adopting sterile TFF-MV filter units with pore sizes of 200 nm cut-off (HansaBioMed Life Sciences; #HBM-TFF-MV). The TFF-MV permeate was further processed by automated TFF, using sterile TFF-EVs filter units with pore sizes of 50 nm cut-off (HansaBioMed Life Sciences; #HBM-TFF-EVs-S). After three sequential washing steps with phosphate buffered saline for enhancing purification from soluble proteins, the EV-containing TFF-EVs retentate was collected and subjected to a final dead-end filtration step, adopting filter units with 0.45 μ m pore size (Sartorius; #16537-----K). EV samples were lyophilized for further downstream analyses. The nanoparticle concentration and size distribution was assessed by Nanoparticle Tracking Analysis (NTA), using ZetaView PMX-120 (software version 8.05.12 SP1) equipped with a 488 nm laser (40 mW power) and a CMOS camera sensor (Particle Metrix, Germany).

EV Tetraspanin-8 detection through ELISA assay: CbEV expression of Tetraspanin-8 (TET8), which have been recently recognized as plant EV--enriched protein markers [7], was revealed using specific antibodies (PhytoAB, #PHY1490S).

Assessment of EV glycosylation pattern by lectin assay: CbEV glycosylation pattern was assessed using the fluorescent lectin assay provided by Vector Laboratories according to its instruction procedure.

Cell culture: skin cells (HaCaT and HDF) and sensory-like neurons were grown in DMEM culture media (Gibco) supplemented with 10% FBS (Hyclone and Gibco) at 37°C and 5% CO₂.

Wound healing: HaCaT or HDF were seeded in a 6well plates (8×10^5 cells/well or 6×10^5 cells/well, respectively) and scratched with a pipette tip after they reached the confluence. Images of cells migration were taken at time 0 and after 16 hours (HaCaT) and 8 hours (HDF). The relative migration of the cells (wound closure area) was calculated using Image J software (T0 and T16/T8 ratios).

Pro-Collagen I, GDF11 and IGF1 detection: ELISA assay was carried out on 4% PFA fixed cells by using specific antibodies (sc-166572, Santa-Cruz Biotechnology; ab124721, Abcam; MA1088, Life technologies).

IL6 and CGRP detection through ELISA Assay: ELISA assay was performed on cell culture media by using commercial kits (88-7066-88, Life technologies; abx257902, Abbexa)

Gene expression analysis by dPCR: Total RNA was extracted using the GenElute Mammalian Total RNA Purification Kit (SIGMA), and EV-derived miRNAs with the RNA Basic kit (HansaBiomed). cDNA synthesis was performed using Wonder RT (Euroclone) for mRNA and the miRCURY LNA RT Kit (QIAGEN) for miRNAs. Digital PCR (QIAcuity, QIAGEN) was carried out with EvaGreen mix following in-house optimized protocols. Gene expression was normalized to HPRT1, while miRNA levels were quantified absolutely.

Microscale thermophoresis: MST experiments were carried out on a Monolith PicoRed system (Nano Temper Technologies, Munchen, Germany) using 60% LED. The labelling of CRD-Gal3 (10µM) was performed with NT-647 reactive dye (30µM) (Nanotemper) incubating the sample for 1h at RT. An equation implemented by the software MO Affinity Analysis3, provided by the manufacturer, was used for fitting normalized fluorescence values at different concentrations of ligands.

3. Results

Isolation and characterisation of CbEVs

EVs were isolated from *Coffea bengalensis* cell culture media (CbEVs) using tangential flow filtration (TFF). Nanoparticle tracking analysis (NTA) estimated an EVs concentration of 4.0×10^{10} particles/mL with a median size of 143 nm (**Figure 1a**). The presence of intact CbEVs in our isolate was validated by ELISA-based detection of plant EV membrane protein marker TET8 (i.e., 2.4 ± 0.4 signal-to-noise ratio relative to $2.5E+8$ particles). Glycan profiling via lectin

assay highlighted pronounced Concavalin A(ConA)- and Ricinus communis agglutinin I (RCA I)-associated fluorescent signals, consistent with the predominant exposure of mannose and N-acetylgalactosamine/galactose residues, respectively, on the membrane surface of CbEVs (**Figure 1b**).

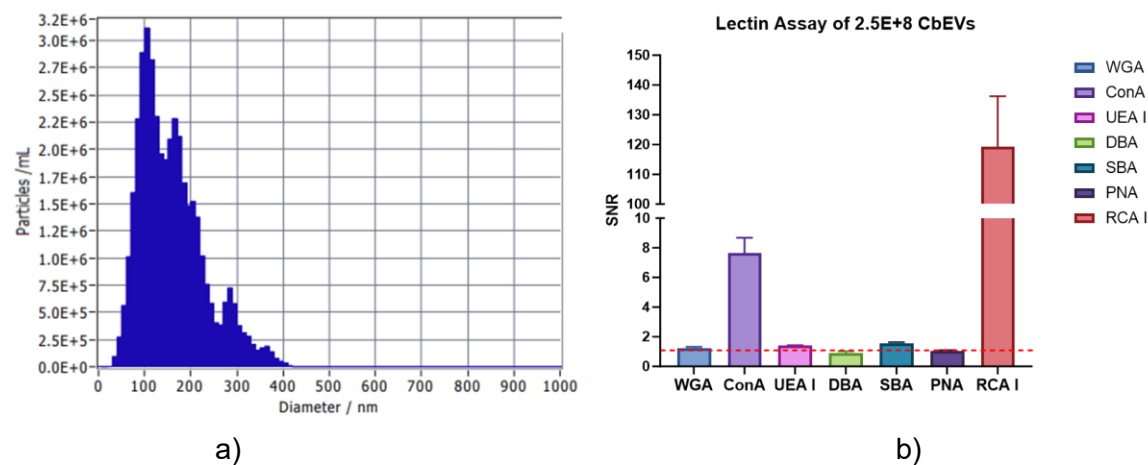


Figure 1. Characterization of CbEV size (a) and glycosylation pattern (b). CbEV size distribution and glycan profile were assessed by NTA and lectin assay, respectively. Lectin assay data are reported as mean \pm SD of two technical replicates. Legend: WGA = Triticum vulgaris (wheat germ) agglutinin; ConA = concavalin A; UEA I = Ulex europaeus agglutinin I; DBA = Dolichos biflorus agglutinin; SBA = soybean agglutinin; PNA = peanut agglutinin; RCA I = Ricinus communis agglutinin I; SNR = signal-to-noise ratio.

CbEVs increased wound healing, collagen synthesis and growth factors production

We investigated the biological activity of CbEVs with focus on skin regeneration properties. In particular, we evaluated the ability of CbEVs in boosting the wound healing process in both keratinocytes and fibroblasts. As shown in **Figure 2**, CbEVs were able to significantly increase the wound healing capacity of keratinocytes, by 50%. Similarly, the effect on fibroblasts migration was increased by 30% (data not shown).

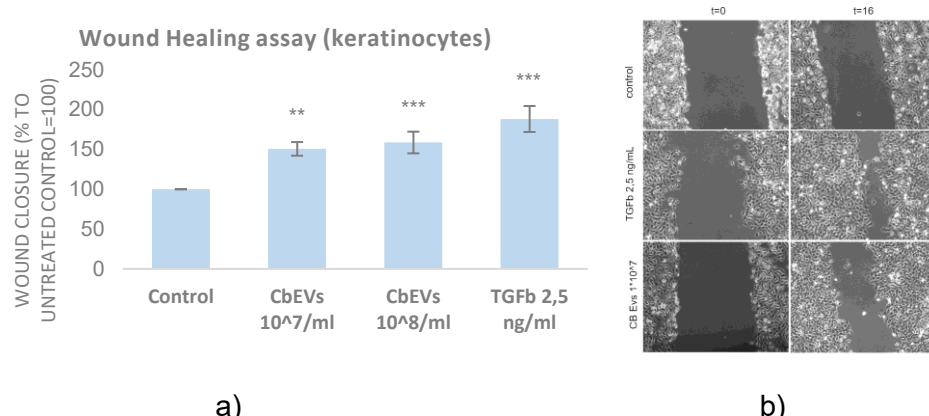


Figure 2. Wound healing assay in HaCaT cells, analysis (a) and raw images (b).

Wound area was measured by ImageJ software. Data represent the average of 3 independent experiments \pm standard deviations with statistical significance determined using Student's t-test (* $p < 0.05$, ** $p < 0.01$ and *** $p < 0.001$).

Furthermore, CbEVs significantly enhanced the synthesis of Pro-collagen 1 (COL1A), GDF11 and IGF1 in fibroblasts (**Figure 3**).

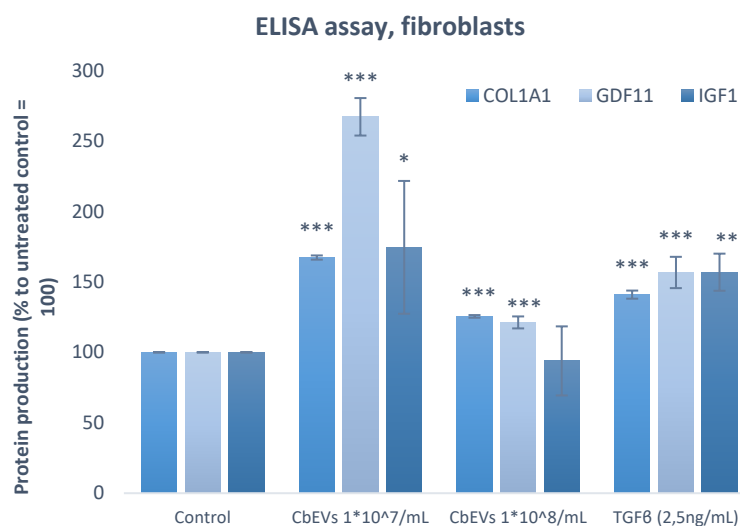


Figure 3. ELISA Assay for COL1A, GDF11 and IGF1 in HDF cells. Data represent the average of 3 independent experiments \pm standard deviations with statistical significance determined using Student's t-test (* $p < 0.05$, ** $p < 0.01$ and *** $p < 0.001$).

Detection of CbEVs miRNAs: miR-159 downregulates IL-33 in human keratinocytes

In order to characterize CbEVs for the presence of specific miRNAs, they were processed and analysed by digital PCR. We detected miR-156, miR-159, miR-166, miR-319 and miR-168. These miRNAs are quite abundant in Plantae [8, 9], but their role in EVs has not been investigated, especially for cosmetic purposes. For this reason, we performed a miR-target prediction analysis [10,11] to identify potential human target genes (listed in **Table 1** along with their quantification and function).

Table 1. CbEVs miRNAs and their predicted human targets

miRNAs	copies/uL	Lenght (nt)	Predicted Target Genes	Pathways involved
miR-156 TGACAGAACAGAGTGAGCAC	8936	20	FFG5, COL4A3, RFX4, RFX5	Skin extracellular matrix, collagen synthesis
miR-159 TTGGATTGAAGGGAGCTCT	84850	20	KLK7, IL-33, RFX3, HDAC4, HDAC6	Skin inflammation, allergy, collagen synthesis, cells senescence
miR-166 TCGGACCAGGCTTCATTCCCC	32	21	FERTK	Skin pigmentation
miR-168 TCGCTTGGTGCAGGTGGGA	132	20	PL1, VDR, DUSP-26, SOX9, SOX2	Skin extracellular matrix, skin protection, inflammation

For the experimental validation, we selected miR-159, which was the most abundant miR detected in CbEVs. Among miR-159 predicted targets, we found IL-33, an alarmin playing a crucial role in neurogenic inflammation and skin diseases, including itching, sensitive skin, psoriasis and atopic dermatitis [12]. Therefore, we evaluated the expression of IL-33 in keratinocytes treated with CbEVs, endogenously carrying miR-159, and also with a miR-159 mimic. As shown in **Figure 4**, IL-33 mRNA was significantly downregulated in either the cells treated with the EVs or with the synthetic miR-159.

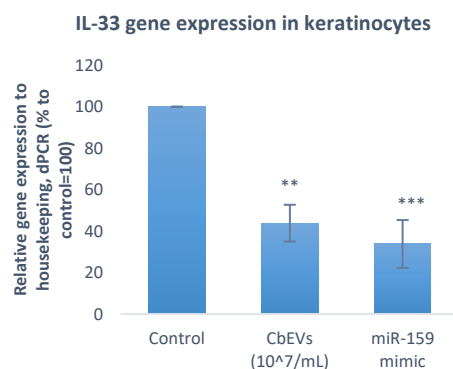


Figure 4. Gene expression analysis of IL-33 in HaCaT cells treated with CbEVs and miR-159 mimic. Data represent the average of 3 independent experiments \pm standard deviations with statistical significance determined using Student's t-test (* $p < 0.05$, ** $p < 0.01$ and *** $p < 0.001$).

We also assessed other miR-159 targets involved in skin inflammation and senescence, such as HDAC4 and HDAC6, and found them downregulated (data not shown). To confirm these effects were miR-159-dependent, we used dPCR to test for miR-159 uptake after CbEV treatment. We detected 122.8 copies/ μL of plant miR-159 in treated cells, while it was absent in controls, confirming EVs internalization and delivery of bioactive cargo.

CbEVs interacts with Galectin-3

Microscale thermophoresis analysis showed that CbEVs interact with Carbohydrate Recognition Domain (CRD) of Galectin-3, a lectin expressed in skin tissue that can trigger inflammatory responses through the release of IL-6, a proinflammatory cytokine also involved in neurogenic inflammation. The recombinant protein was prepared in accord to Di Gaetano et al [13].

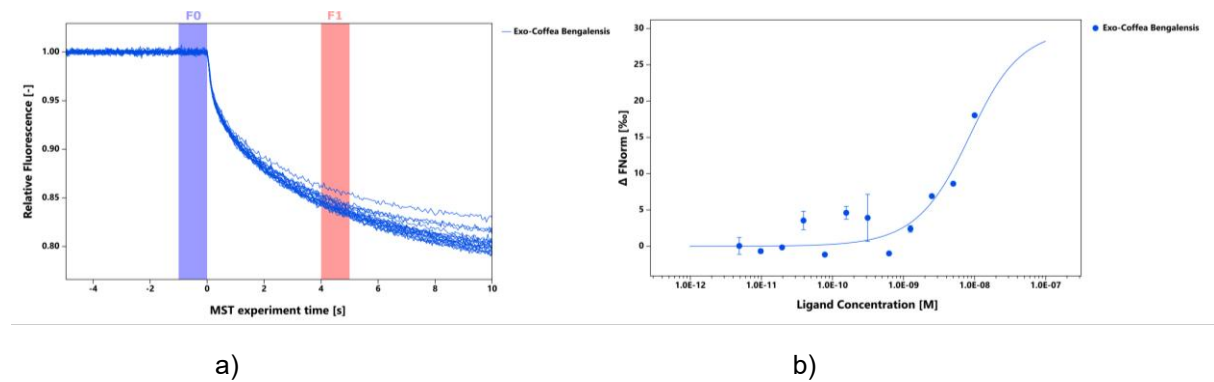


Figure 6. Microscale thermophoresis of CbEVs and recombinant CRD-Gal3 interaction. a) MST traces of titrations of CbEVs against CRD-Gal3; F0 and F1 correspond to the fluorescence of unbound state and bound state respectively. (b) Binding curve graph obtained plotting normalized fluorescence of CRD Gal-3 in presence of increasing concentrations of CbEVs (18 nM – 0,5 pM).

CbEVs mitigates neurogenic inflammation modulating keratinocytes gene expression

To determine if the interaction between CbEVs and Galectin-3 influences inflammation in keratinocytes., HaCaT cells were treated with rGal3 and with CbEVs and IL6 expression was evaluated. As reported in **Figure 7**, Gal3 induced an increase in IL6 gene expression by 20% but the presence of CbEVs attenuates this effect by more than 40% resulting in a lower stress state compared to the control cells.

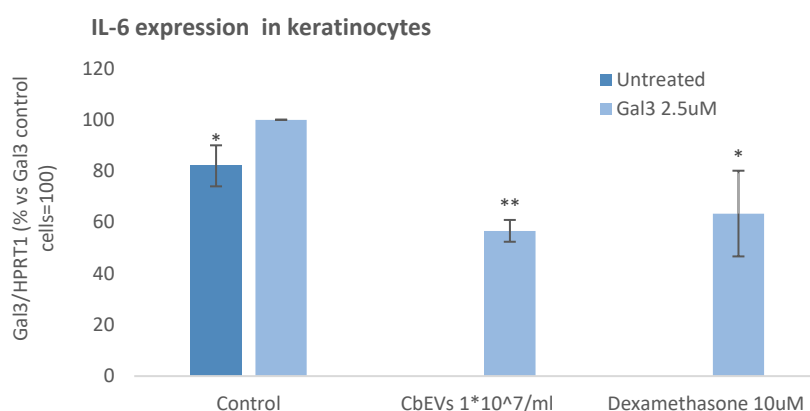


Figure 7. Gene expression analysis in HaCaT cells stressed with Gal3 and treated with CbEV or Dexamethasone. Data represent the average of 3 independent experiments \pm standard deviations with statistical significance determined using Student's t-test (* $p < 0.05$ and ** $p < 0.01$).

To investigate whether CbEVs were able to mitigate inflammation even in presence of other inflammatory conditions we evaluated their effect on gene expression of IL-6 , IL-8 and PAR-2, in keratinocytes stressed with a cocktail of pro-inflammatory cytokines. As shown in **Figure 8**, CbEVs were able to significantly reduce PAR-2 and IL-8 in cytokines-stressed cells. As positive control, 10μM of dexamethasone was used [14].

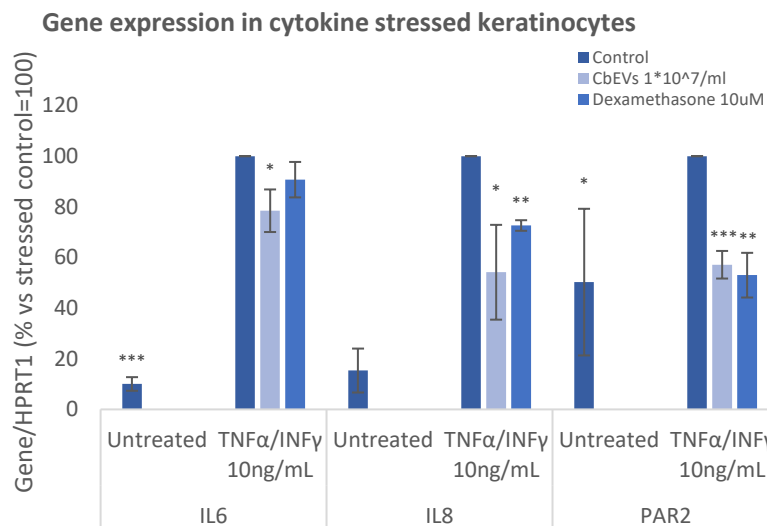


Figure 8. Gene expression analysis of inflammation markers in HaCaT cells treated with pro-inflammatory cytokines. Data represent the average of 3 independent experiments \pm standard deviations with statistical significance determined using Student's t-test (*p < 0.05, **p < 0.01 and ***p < 0.001).

CbEVs mitigates neurogenic inflammation modulating keratinocytes and neurons crosstalk

To further confirm the role in modulation neurogenic inflammation, we performed a co-culture experiment between keratinocytes and sensory-like neurons and quantified the release of both IL-6 protein and CGRP neuropeptide from them. For CGRP analysis, we also included a stress with its natural inducer, capsaicin. We observed that CbEVs were able to significantly reduce the release of both IL-6 and CGRP (**Figure 9**).

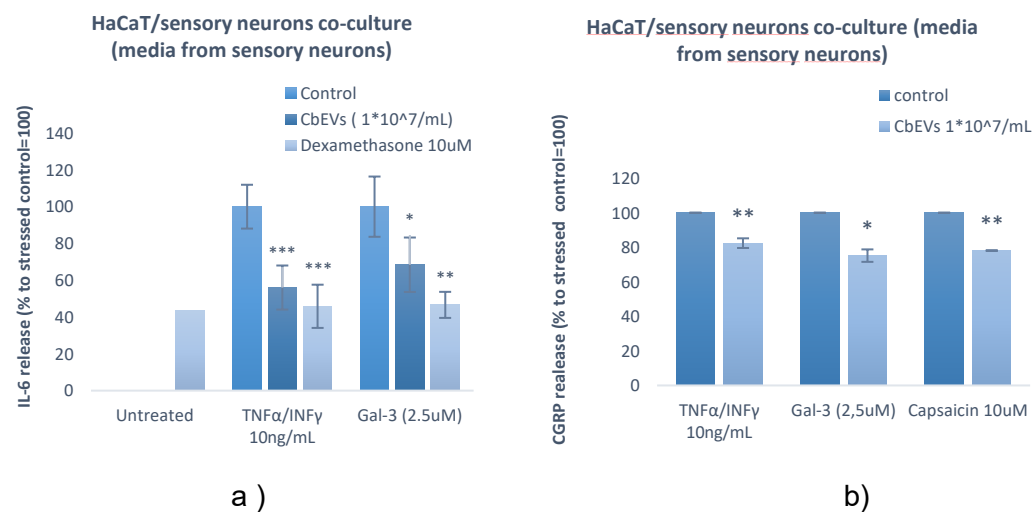


Figure 9. ELISA assay for IL-6 (a) and CGRP (b) proteins from sensory-like neurons' culture media. Data represent the average of 3 independent experiments \pm standard deviations with statistical significance determined using Student's t-test (*p < 0.05, **p < 0.01 and ***p < 0.001).

Taken together these data demonstrated that CbEVs modulates neurogenic inflammation and this is likely due to the interaction with galectin-3 but also to the presence of a specific miRNA that regulates IL33 expression.

4. Discussion

This study provides novel insight into the effective potential of *Coffea bengalensis*-derived extracellular vesicles (CbEVs) in the context of skin regeneration and skin inflammation. These results underscore the capacity of CbEVs to modulate intercellular communication, immune response, and pigmentation pathways through intricate molecular interactions, highlighting their potential as bioactive agents for skin care application. A key finding of this work is the interaction between CbEVs and Galectin-3 (Gal3), a β-galactoside-binding lectin, extensively studied for its involvement in cutaneous immunity and inflammation [15]. In the skin, it is expressed in keratinocytes, hair follicles, sebaceous and sweat glands, and fibroblasts [16]. The binding of CbEVs to Gal3's carbohydrate recognition domain (CRD) suggests a selective and biologically relevant interaction that modulates inflammatory milieu. In the same vein, it goes the reduction in IL6 and IL8 release by inflamed keratinocytes treated with CbEVs. Beyond cytokines, the study highlights a regulatory role for CbEVs in the expression of protease-activated receptor 2 (PAR2), a G protein coupled receptor involved in different skin pathway like itching or pigmentation [17]. PAR2 is overexpressed in conditions like atopic dermatitis in which exacerbates neuro-epidermal communication or in vitiligo and melasma in which it induces melanosome uptake from keratinocytes. One typical consequence of an inflammatory condition is the formation of post-inflammatory hyperpigmented lesions [18]. Our data demonstrated that CbEVs regulates the expression of PAR2 in inflammatory keratinocytes suggesting a potential use of this exosomes to regulate pigmentation. Furthermore, CbEV regulates also melanin synthesis in melanocytes (data not shown) contributing to pigmentation regulation. In addition to cytokine and pigment regulation, this study reveals the impact of CbEVs on neurogenic inflammation, a critical and often overlooked component of skin pathology. The identification of a CbEVs-associated microRNA capable of downregulating IL33, an alarmin released by keratinocytes and immune cells in particularly stressed conditions [12], represents a significant advancement. In co-culture *in vitro* systems, stressed keratinocytes treatment with CbEVs results in a significant decrease in IL6 and neuropeptide CGRP release from sensory neurons. This demonstrated a role of CbEVs in regulate communication between keratinocytes and sensory neurons and a global effect in reducing neurogenic inflammation. Given that CGRP not only potentiates inflammation but also enhances melanogenesis [19], CbEVs exert a comprehensive regulatory influence spanning immune, neural and pigmentary pathway.

5. Conclusion

CbEVs act as multifaceted modulators of skin physiology regulating key processes for skin regeneration like wound healing, Extracellular Matrix protein and Growth factors synthesis. By targeting key molecules like Gal3, PAR2, IL-6, IL-33, and CGRP, CbEVs influence a broad spectrum of skin processes including inflammation, pigmentation, and neuron-keratinocyte signaling. Therefore, CbEVs are potent, natural plant component able to regulate skin conditions like inflammation, pigmentation alteration and neurogenic skin issues. Future research should focus on validating these findings in in vivo models and clinical settings.

6. References

- [1] <https://doi.org/10.3390/ijms25116199>
- [2] <https://doi.org/10.1016/j.bbih.2021.100361>
- [3] <https://doi.org/10.1172/jci.insight.142067>
- [4] <https://doi.org/10.1016/j.acthis.2012.11.010>
- [5] <https://doi.org/10.1002/mco2.741>
- [6] Cosmet. Toilet. 2011, 126, 644–650
- [7] <https://doi.org/10.1002/jev2.12283>
- [8] <https://doi.org/10.1080/15592324.2021.1915590>
- [9] [https://doi.org/10.1016/j.scienta.2023.112010.](https://doi.org/10.1016/j.scienta.2023.112010)
- [10] <https://doi.org/10.1186/s13059-019-1629-z>
- [11] <https://doi.org/10.1093/nar/gkz757>
- [12] <https://doi.org/10.1016/j.coi.2014.09.004>
- [13] <https://doi.org/10.3390/ijms23052581>
- [14] <https://scispace.com/journals/journal-of-pharmacology-and-experimental-therapeutics-zdvzfms0>
- [15] <https://doi.org/10.1016/j.dsi.2012.10.002>
- [16] <https://doi.org/10.1016/j.jdermsci.2011.07.008>
- [17] <https://doi.org/10.1111/exd.13936>
- [18] <https://doi.org/10.1111/pcmr.13038>
- [19] <https://doi.org/10.3390/ijms24055001>